Exact Solution to Optical-Model Equations for Quasi-Elastic (p,n) Reactions*

ERVIN H. SCHWARCZ
Lawrence Radiation Laboratory, University of California, Livermore, California
(Received 12 May 1966)

The coupled optical-model equations describing quasi-elastic (p,n) reactions are solved exactly and the results are compared with distorted-wave Born approximation (DWBA) solutions. It is shown that for reasonable values of the isobaric potential the DWBA deviates only slightly from the exact solution. Fits to experimental data are presented for $Ti^{48}(p,n)V^{48}$, $V^{51}(p,n)Cr^{51}$, and $Cr^{52}(p,n)Mn^{52}$.

THE optical-model equations proposed by Lane[1] to explain the neutron spectra found by Anderson *et al.*[2] in (p,n) reactions included a term of the form $(U_1/A)\mathbf{t}\cdot\mathbf{T}$. This term, among other things, brings about a charge exchange so that the process can be thought of as quasi-elastic. The solution to this optical-model equation is complicated by the fact that the neutron and proton channels are coupled, and that if no approximations are made, the equations cannot be decoupled by any transformation.

Two approximate solutions have been made. The first, which was investigated by Hodgeson and Rook,[3] neglected the Coulomb potential and the Coulomb energy difference between the target and residual nuclei. In this case, the equations decouple and can be numerically solved by existing one-channel, optical-model codes. The second approximate solution was a DWBA calculation carried out by Satchler *et al.*[4] Both approximations led to the conclusion that the (p,n) cross section scales as the square of the strength of the isobaric potential U_1. Further, Satchler *et al.*,[4] in fitting the experimental results of Anderson *et al.*,[2] found values for the isobaric parameters to give best fits.

In view of the work of Robson,[5] Fox *et al.*,[6] and Richards *et al.*,[7] who have shown the importance of this optical model to (p,p) scattering and its consequent usefulness as a spectroscopic tool, it was thought important to solve the coupled equations exactly without neglecting the Coulomb potential or the Coulomb energy difference between target and residual nuclei. This would be done to check on the conclusions drawn from the approximate solutions relating to the proportionality of the (p,n) cross section to the square of U_1 and the actual values of the parameters.

Solution of the equations. The coupled equations, as given by Lane,[1] are

$$\left(T+U_0+V_c-\frac{1}{2A}T_0U_1\right)\Psi_p+\frac{1}{A}\left(\frac{T_0}{2}\right)^{1/2}U_1\Psi_n=0,$$

$$\left[T+U_0+\Delta_c+\frac{1}{2A}(T_0-1)U_1\right]\Psi_n+\frac{1}{A}\left(\frac{T_0}{2}\right)^{1/2}U_1\Psi_p=0,$$

where T is the kinetic energy operator. The boundary conditions state that the proton asymptotic wave function should be the incident wave plus outgoing scattered wave while the neutron asymptotic wave function should consist only of the outgoing wave, there being no incident neutron wave.

Using the standard partial-wave decomposition, the boundary conditions for the lth partial wave are

$$\Psi_l{}^{p\pm}\sim F_l(\eta,k_pr)+C_l{}^{p\pm}[G_l(\eta,k_pr)+iF_l(\eta,k_pr)], \quad (1)$$

$$\Psi_l{}^{n\pm}\sim C_l{}^{n\pm}[-k_nry_l(k_nr)+ik_nrj_l(k_nr)]. \quad (2)$$

If the continuity of the logarithmic derivative is imposed on Ψ_p, one obtains a proper asymptotic proton wave function. This cannot be applied to the neutron

TABLE I. (p,n) cross sections as a function of isobaric potential strength.

U_1 (MeV)	$U_1^2/20^2$	$\sigma_{\text{surf}}(90°, U_1)$	$\frac{\sigma_{\text{surf}}(90°, U_1)}{\sigma_{\text{surf}}(90°, 20\text{ MeV})}$	% deviations
20		0.012		
40	4	0.046	3.83	4.25
60	9	0.103	8.58	4.66
80	16	0.181	15.08	5.75
100	25	0.279	23.25	7.00
120	36	0.395	32.92	8.56
140	49	0.527	43.92	10.37
160	64	0.671	55.92	12.63
		$\sigma_{\text{vol}}(90°, U_1)$	$\frac{\sigma_{\text{vol}}(90°, U_1)}{\sigma_{\text{vol}}(90°, 20\text{ MeV})}$	
20		0.029		
40	4	0.116	4.00	0.
60	9	0.259	8.93	0.78
80	16	0.454	15.66	2.13
100	25	0.696	24.00	4.00
120	36	0.980	33.79	6.14
140	49	1.296	44.69	8.80
160	64	1.637	56.44	11.81

* Work performed under the auspices of the U. S. Atomic Energy Commission.

[1] A. M. Lane, Nucl. Phys. **35**, 676 (1962).
[2] J. D. Anderson and C. Wong, Phys. Letters **7**, 250 (1961); **8**, 442 (1962).
[3] P. E. Hodgson and J. R. Rook, Nucl. Phys. **37**, 632 (1962).
[4] G. R. Satchler, R. M. Drisko, and R. H. Bassel, Phys. Rev. **136**, B637 (1964).
[5] D. Robson, Phys. Rev. **137**, B505 (1965).
[6] J. D. Fox, C. F. Moore, and D. Robson, Phys. Rev. Letters **12**, 198 (1964).
[7] P. Richards, C. F. Moore, D. Robson, and J. D. Fox, Phys. Rev. Letters **14**, 343 (1964).

wave function, however, since the absence of an incident neutron part would result in cancellation of $C_l{}^{n\pm}$. Therefore, since the method used to satisfy the boundary conditions in the one-channel optical model does not work here, a brief description of the method used is presented.

The method used was to solve the coupled equations twice, with different initial conditions chosen so as to give two independent solutions. The general solutions are a linear combination of the two independent solutions:

$$\Psi^p = A_1\Psi_1{}^p + A_2\Psi_2{}^p, \quad \Psi^n = A_1\Psi_1{}^n + A_2\Psi_2{}^n.$$

It is important to note that the same constants A_1 and A_2 are used in the proton and neutron wave functions, since if $\Psi_1{}^p$ and $\Psi_1{}^n$ are solutions for given initial conditions, then $A_1\Psi_1{}^p$ and $A_1\Psi_1{}^n$ are also solutions.

Using partial waves, in the usual manner, one can write the boundary conditions

$$A_{1,l}{}^{\pm}\Psi_{1,l}{}^{p\pm} + A_{2,l}{}^{\pm}\Psi_{2,l}{}^{p\pm} = F_l(\eta,k_p r) + C_l{}^{p\pm}[G_l(\eta,k_p r) + iF_l(\eta,k_p r)],$$

$$A_{1,l}\Psi_{1,l}{}^{n\pm} + A_{2,l}{}^{\pm}\Psi_{2,l}{}^{n\pm} = C_l{}^{n\pm}[-k_n r y_l(k_n r) + ik_n r j_l(k_n r)].$$

These equations, together with their derivatives, can then be solved as a system of four complex equations for the four complex unknowns $A_{1,l}{}^{\pm}$, $A_{2,l}{}^{\pm}$, $C_l{}^{p\pm}$, and $C_l{}^{n\pm}$.

In Table I we show the cross sections for different strengths of the pure volume and pure surface isobaric potentials for $V^{51}(p,n)Cr^{51}$. The nonisobaric parameters used in this table are those considered reasonable for (p,p) scattering and not necessarily the best values for fitting the experimental data. It is seen that for values of U_1 currently thought to be reasonable ($U_1 \cong 100$ MeV), the proportionality of the (p,n) cross sections to $U_1{}^2$ is reasonable, although the deviation starts to increase rapidly for higher values of U_1.

To compare the exact solutions with Satchler's, we ran the problem for $Ti^{48}(p,n)V^{40}$ with the following parameters ($R_0 = 1.25A^{1/3}$):

(1) Central real potential: $-49.4/[1+e^{(r-R_0)/0.65}]$ MeV,
(2) Central imaginary potential: $-10.0e^{-[(r-R_0)/0.98]^2}$ MeV,
(3) Spin-orbit factor: 25.5 (corresponding to 7 MeV),
(4a) Isobaric potential: $81.0/[1+e^{(r-R_0)/0.65}]$ (volume),
(4b) Isobaric potential: $84.0e^{-[(r-R_0)/1.36]^2}$ (surface).

The strength of 84 MeV for the surface isobaric interaction was obtained by inserting Satchler's value of 96 MeV in his formula (15) and then dividing by four, since Satchler's isobaric form factor when multiplied by four approximates case (4b) above.

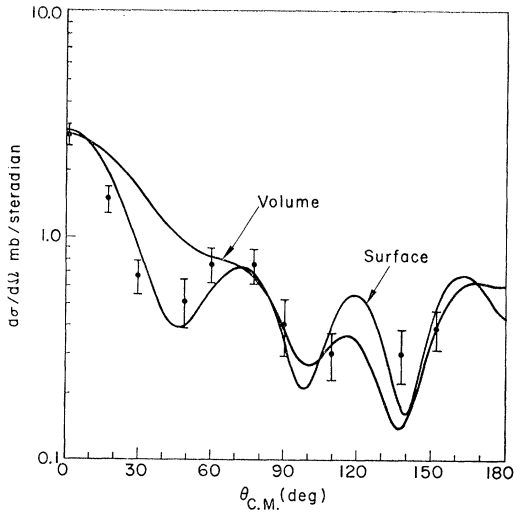

FIG. 1. $Ti^{48}(p,n)V^{48}$ differential cross section for both volume and surface isobaric potential to compare with DWBA results.

While it is true in general that when comparing the DWBA and exact solutions, the parameters used in the exact solution should be readjusted from the DWBA so as to give the same elastic scattering, in this case the coupling is sufficiently weak so that the elastic scattering is changed very little.

The results of our calculation are given in Fig. 1. If we compare our results with those in Satchler's paper,[4] we see that the general shape of the DWBA follows that of the exact calculation for both volume and surface isobaric potential. Quantitatively, however, the exact solution for volume isobaric potential predicts higher cross sections for larger angles than does the DWBA. Although for all nuclei investigated, surface isobaric potentials give better agreement than volume isobaric potentials, the exact volume isobaric potential comes closer to the experimental values than does the

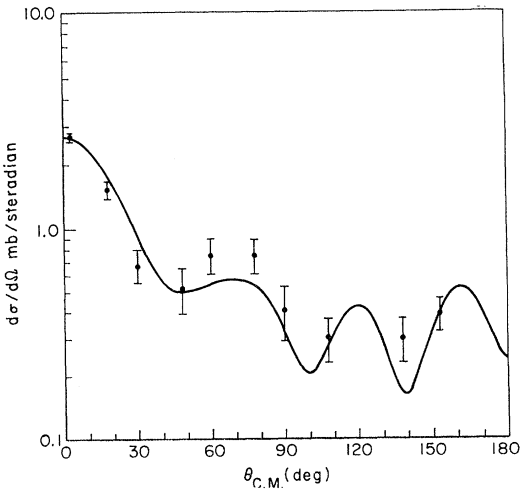

FIG. 2. $Ti^{48}(p,n)V^{48}$ differential cross section.

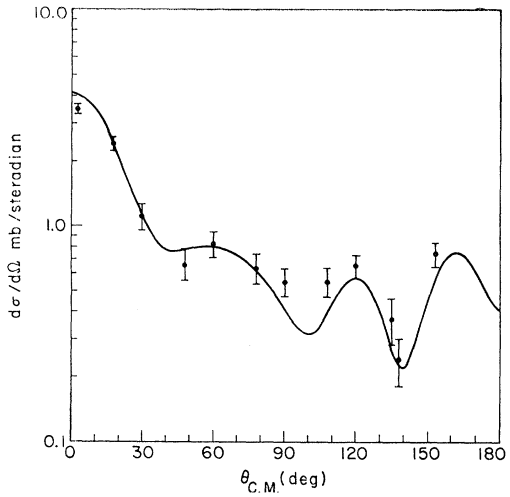

FIG. 3. $V^{51}(p,n)Cr^{51}$ differential cross section.

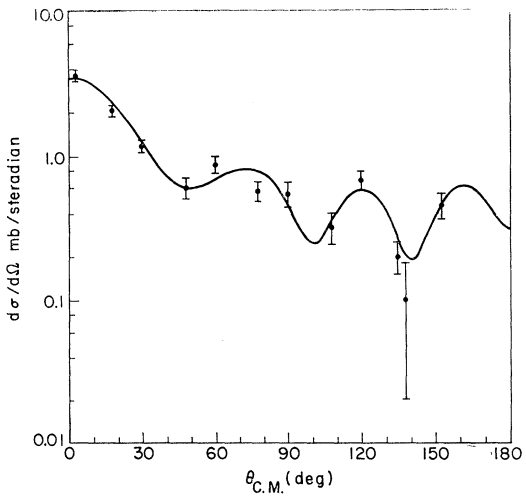

FIG. 4. $Cr^{52}(p,n)Mn^{52}$ differential cross section.

DWBA with volume isobaric potential. This difference between the exact and DWBA solutions is not so great for surface isobaric potential.

The preliminary best fit for $Ti^{48}(p,n)V^{48}$, $V^{51}(p,n)Cr^{51}$, and $Cr^{52}(p,n)Mn^{52}$ is shown in Figs. 2, 3, and 4. Although the results are still preliminary, we seem to be getting a better fit with a small admixture of volume isobaric potential to a predominantly surface isobaric potential. Also, a charge-exchange radius parameter slightly larger than the usual nuclear radius parameter of 1.25 F seems to be preferred.

The form factors used in these figures are

Central real potential: Wood-Saxon (diffuseness parameter = 0.65, radius = $1.25A^{1/3}$),

Central imaginary potential: Surface-centered Gaussian (width = 0.98),

Isobaric potential (volume): Wood-Saxon (diffuseness parameter = 0.65, radius = 1.27),

Isobaric potential (surface): Gaussian (width = 1.05, radius = 1.27).

The parameters are

	Fig. 2	Fig. 3	Fig. 4
Central real potential:	−54.0 MeV	−54.0 MeV	−50.0 MeV
Central imaginary potential:	−12.0 MeV	−12.0 MeV	−11.0 MeV
Spin-orbit parameter:	27.7	27.7	27.7
Surface isobaric potential:	110 MeV	140 MeV	130 MeV
Volume isobaric potential:	10 MeV	0 MeV	10 MeV

The author would like to thank Dr. Joseph Lepore and Dr. Robert Riddell for helpful discussions.